Image Denoising Method for Unknown Noise Based on 2-D FWT with Optimal Fractional Order

Yuanyuan Jiang
College of Automation Engineering, Nanjing University of Aeronautics and Astronautics, Nanjing, China;
Anhui University of Science and Technology, Huainan, China
Email: jyyll672@163.com

Youren Wang and Hui Luo
College of Automation Engineering, Nanjing University of Aeronautics and Astronautics, Nanjing, China
College of engineering, Nanjing Agriculture University, Nanjing, China

***Abstract*—The optimal fractional order should be determined for image denoising by 2-D fractional wavelet transform (FWT). However, the actual application environment is complex, and the input image has already been polluted by unknown noise frequently in the process of capture and transmission. It is impossible to get the optimal fractional order on the basis of the objective evaluation standard in existence. Therefore, in view of the unknown image noise, a method to get the estimated value of optimal fractional order is put forward. Firstly, new objective evaluation standards for image denoising in fractional wavelet domain are defined, and its optimal value is obtained based on noise estimation. Then the optimal estimated fractional order is gained. The experiment results show that, 2-D FWT with the optimal fractional order can be selected reasonably and the unknown image noise can be filtered effectively in the estimated optimal fractional wavelet domain.**

***Index Terms*—image denoising, fractional wavelet transforms, the optimal fractional order, noise estimate**

I. INTRODUCTION

A. Historical Perspective

Images are often corrupted with noise during image acquisition and image transmission [1]. To improve the image quality and meet the need of follow-up image processing, image denoising has become an important work in image pre-processing. In recent years, image denoising methods are emerging one after another. Several classes of denoising algorithms such as nonlocal means [2], [3], wavelets [4], [5], [6], [7], [8], and total variation (TV) [9], [10], [11] have all achieved much success. These algorithms are based on different theories, and all show good performance in denoising. When denoising an image, the TV method makes use of the geometric features of the image, the wavelet method makes use of the statistical features of the coefficients, and the nonlocal means method makes use of the redundancy in the image texture features [12].

Fourier transform (FT) converts a signal from time versus amplitude to frequency versus amplitude. FT is the time–frequency representation of the signal. The conventional FT can be visualized as a change in representation of the signal corresponding to a counterclockwise rotation of the axis by an angle $\pi/2$. Two successive rotations of the signal through $\pi/2$ will result in an inversion of the time axis. FT has some drawbacks like it does not give any information about the occurrence of the frequency component at a particular time and is not applicable for nonstationary signals. To overcome this problem, researchers came up with the short-time FT (STFT) [13]. In STFT, a moving window is applied to the signal, and then the FT is applied to the signal within the window as the window is moved over the whole real line.Although STFT has rectified almost all the limitations/drawbacks of FT, but still in some cases STFT is also not applicable as in the case of real signals having low frequencies of long duration and high frequencies of short duration. Such signals could be better described by a transform which has a high frequency and low time resolution at low frequencies and a low frequency and high time resolution at high frequencies. In these type of situations, wavelet transform can provide a better description of the signal (image) instead of STFT. Wavelets [14] are basically functions that are localized in frequency around a central value and are limited in time. Hence, wavelets are different from the functions used in Fourier analysis since neither they have a constant waveformnor they are of finite support. Wavelets exhibit constant shape because they are generated from only one function [15].

As a very useful tool for multi-resolution and time-frequency analysis, wavelet transform (WT) has been widely studied and applied in image processing [16-17]. The Fractional Wavelet Transform (FWT) has become a new research topic in signal processing, which extend the

Corresponding author: Yuanyuan Jiang, jyyll672@163.com

doi:10.4304/jcp.9.2.412-419

WT to a time-generalized frequency domain called fractional domain [18].

B. Purpose and Contribution

FWT considers parameter $p \in [0,1]$ as the fractional order, and can analyze signals in fractional domain which make signal processing more flexible. With different fractional orders, transformed signals perform various characteristics [18]. Moreover, in fractional domain, the fractional order is uncertain. We must to determine the optimal fractional order firstly. Currently, the selection of the optimal fractional order is according to the evaluation criteria of image denoising, which needs original image without noise. However, images are often corrupted with noise in complicated working environment and the noise is uncertain. Thus, a novel method for unknown noise is presented to gain the optimal fractional order.

The paper is organized as follows. Section II gives the basic background, primarily the theory of fractional Fourier, wavelet transform and fractional wavelet transform. Section Ⅲ gives the overview of the 2-D FWT. This section also illustrates the procedure of 2-D FWT. In section Ⅳ, noise estimation method is discussed. The method of the optimal fractional order is introduced in section Ⅴ and the experiment details and results are discussed in Section Ⅵ. Finally, conclusions are presented.

II. Preliminaries

This section gives the basic background, primarily the theory of fractional Fourier, wavelet transform and fractional wavelet transform which is as follows [19].

A. Fractional Fourier Transform

The concept of Fractional Fourier transform (FRFT) is introduced by Victor Namias in 1980 by generalizing Fourier transform. It is also called rotational Fourier transform or angular Fourier transform since it depends on a parameter a which is interpreted as a rotation by an angle α in the time-frequency plane. This parameter α is called the transform order/fractional order. Mathematically, α -order fractional Fourier transform of the function $f(t)$ is defined as:

$$F(x) = F^{\alpha}[f(t)](x) = \int_{-\infty}^{\infty} K_{\alpha}(t,x) f(t) \mathrm{d}t \tag{1}$$

where α is called the transform order and $K_{\alpha}(t,x)$ is the fractional Fourier transform kernel and is given as:

$$K_{\alpha}(t,x) = \begin{cases} \sqrt{1-i\cot\alpha}\, e^{\left(i\frac{t^2+x^2}{2}\cot\alpha - ixt\csc\alpha\right)}, \alpha \neq n\pi \\ \delta(t-x), \alpha = 2n\pi \\ \delta(t+x), \alpha = 2n\pi \pm \pi \end{cases} \tag{2}$$

where n is a given integer. Further, rearranging the kernel $K_{\alpha}(t,x)$ as:

$$K_{\alpha}(t,x) = C_{\alpha} k_{\alpha}(t,x) e^{-itx\csc\bar{\alpha}} \tag{3}$$

where $\bar{\alpha} = \alpha\pi/2$, $k_{\alpha}(t,x) = e^{\frac{i}{2}\left(t^2+x^2\right)\cot\bar{\alpha}}$ and $C_{\alpha} = \dfrac{e^{-\frac{i}{2}\left(\frac{\pi}{2}\mathrm{sgn}(\sin\bar{\alpha})-\bar{\alpha}\right)}}{\sqrt{2\pi\left|\sin\bar{\alpha}\right|}}$.

It is clear that if $\bar{\alpha} = \alpha\pi/2$ then $C_{\alpha} = \sqrt{\dfrac{1-i\cot\alpha}{2\pi}}$. This can be verified easily with the use of the identity $\dfrac{1}{\sqrt{\pi\left(1-e^{-2i\pi}\right)}} = \dfrac{e^{-\frac{i}{2}\left(\frac{\pi}{2}\mathrm{sgn}(\sin\bar{\alpha})-\bar{\alpha}\right)}}{\sqrt{2\pi\left|\sin\bar{\alpha}\right|}}$. Similarly, if $\sin\bar{\alpha} = 0$ then by a limiting process the kernel reduces to a Dirac delta $(\delta(x \pm t))$. More details on the rearrangement can be found in. Now, let us consider a set of normalized n -order Hermite functions with unit variance, i.e.

$$H_n(t) = \frac{1}{\sqrt{2^n n!\sqrt{\pi}}} h_n(t) e^{-t^2/2} \tag{4}$$

where $h_n(\bullet)$ is the n th-order Hermite polynomial and given by

$$h_n(t) = (-1)^n e^{t^2} D^n\left(e^{-t^2}\right) \tag{5}$$

where D^n represents the n th-order derivative with respect to t. Now, using Mehler's Hermite Polynomial formula,

$$K_{\alpha}(t,x) = \sum_{n=0}^{\infty} \lambda_n^{\alpha} H_n^*(x) H_n(t) \tag{6}$$

where $\lambda_n = e^{-in\pi/2}$. If the (6) is observed then it is clear that it is the spectral expansion of the transform kernel K_{α} with eigenvalues λ_n^{α} and $H_n(t)$ that acts as corresponding eigenvectors. Now, using (1) and (6)

$$F(x) = \sum_{n=0}^{\infty} e^{-in\alpha} H_n^*(x) \int_{-\infty}^{\infty} H_n(t) f(t) \mathrm{d}t \tag{7}$$

where $\alpha = a\pi/2$. Further, (7) also interprets that FRFT is a weighting sum of the Hermite functions. The FRFT of a signal exists under the same conditions in which its Fourier transform exists. The inverse FRFT can be visualized as the FRFT with transform order $-\alpha$. The main property of FRFT is that the signal obtained is in purely time domain if transform order (α) is 0 and in purely frequency domain if transform order (α) is $\pi/2$. It is important to point out that various α values provide transformations with distinctive properties. Hence, α can be adjusted in many applications to provide enhanced results in comparison to other existing methods.

B. Wavelet Transform (WT)

Wavelets are basically functions that are localized in frequency around a central value and that are limited in time, i.e., they are of finite support and hence are localized in time around a central value. Therefore, wavelets are different from the functions that are used in

Fourier analysis in the sense that they have neither constant waveform nor finite support. The wavelets are generated from a single function called mother wavelet function by dilating and translating it in the time parameter. Mathematically, the mother wavelet function w is defined as.

$$\Psi_{s,\tau}(t)=\frac{1}{\sqrt{s}}\Psi\left(\frac{t-\tau}{s}\right) \tag{8}$$

where s and τ are the parameters which are used to control dilation and translation respectively. The mother wavelet function always satisfies the two conditions given as

$$\int_{-\infty}^{\infty}\Psi_{s,\tau}(t)\mathrm{d}t=0$$
$$\int_{-\infty}^{\infty}\left|\Psi_{s,\tau}(t)\right|^2\mathrm{d}t=1 \tag{9}$$

here first part of (9) shows the zero mean condition whereas second part shows the square norm one condition. On the basis of mother wavelet function Ψ, the wavelet transform of a function $f(t)$ is defined by the following equation.

$$W(s,\tau)=\int_{-\infty}^{\infty}f(t)\Psi_{s,\tau}(t)\mathrm{d}t \tag{10}$$

The above equation suggests that the wavelet transform is the correlation of the input signal with a time-reversed version of Ψ rescaled by a factor of s. Given the wavelet transform of a function it is possible to restore the signal perfectly using the inverse wavelet transform defined as.

$$f(t)=\frac{1}{C_\Psi}\int_{-\infty}^{\infty}\int_{-\infty}^{\infty}W_f(s,\tau)\Psi_{s,\tau}(t)\frac{\mathrm{d}s\mathrm{d}\tau}{s^2} \tag{11}$$

where $C_\Psi\int_{-\infty}^{\infty}\frac{\left|\hat{\Psi}(u)\right|^2}{|u|^2}\mathrm{d}u$ with $\hat{\Psi}(u)$ as the Fourier Transform of $\Psi(t)$. It is important to note that in (8)-(11), the wavelet basis functions are not specified. This is a difference between the wavelet transform and the Fourier transform, or other transforms. The theory of wavelet transforms deals with the general properties of the wavelets and wavelet transforms only. It defines a generic framework within which one can design wavelets as per requirements of the application.

C. Fractional Wavelet Transform (FWT) [20]

To adapt the localization existing in the FRFT to the localization existing in the wavelet components, the following definition for the FWT: performing a FRFT with the optimal fractional order p over the entire input signal and then performing the conventional wavelet decomposition. For reconstruction, one should use the conventional inverse wavelet transform and then carry out a FRFT with the fractional order of $-p$ to return back to the plane of the input function. A flowchart of the FWT is illustrated in Fig. 1. The fractional order p of the FWT is determined in such a way that the mean-square error between the original input and the reconstructed input is minimal. Indeed, this optimization step may be long and be followed by many calculations.

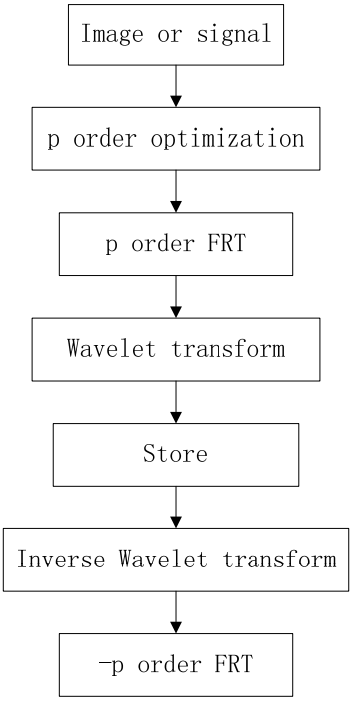

Figure 1. Flowchart of the FWT

Mathematically, the FWT may be formulated as follows:

$$W^{(p)}(a,b)=\int_{-\infty}^{\infty}\int_{-\infty}^{\infty}B_p(x,x')f(x')h_{ab}^{*}(x)\mathrm{d}x'\mathrm{d}x \tag{12}$$

where $W^{(p)}(a,b)$ is the FWT and B_p is defined by (13) and (14). Note that, for $p=1$, the FWT becomes the conventional wavelet transform.

$$B_p(x,x')=\sqrt{2}\exp\left[-\pi\left(x^2+x'^2\right)\right]$$
$$\times\sum_{n=0}^{\infty}\frac{i^{-pn}}{2^n n!}H_n\left(\sqrt{2\pi}x\right)H_n\left(\sqrt{2\pi}x'\right) \tag{13}$$

where H_n is a Hermite polynomial of order n, or, according to the bulk optics definition.

$$B_p(x,x')=\frac{\exp\left[-i\left(\frac{\pi\,\mathrm{sgn}(\sin\phi)}{4}-\frac{\phi}{2}\right)\right]}{|\sin\phi|^{1/2}\exp\left[i\pi\frac{x^2+x'^2}{\tan\phi}-2i\pi\frac{xx'}{\sin\phi}\right]} \tag{14}$$

where $\phi=\pi p/2$.

The formula for backreconstructing the input is

$$f(x)=$$
$$\frac{1}{C}\int_{-\infty}^{\infty}\int_{-\infty}^{\infty}\int_{-\infty}^{\infty}\frac{1}{a^3}W_p(a,b)B_{-p}(x,x')h\left(\frac{x'-b}{a}\right)\mathrm{d}a\mathrm{d}b\mathrm{d}x' \tag{15}$$

And the hybrid FWT will then be

$$f(x)=\frac{1}{C}\sum_{n=-\infty}^{n=\infty}\int_{-\infty}^{\infty}\int_{-\infty}^{\infty}\frac{1}{2^{2n}}W^{(p)}\left(2^{2n},b\right)\times B_{-p}(x,x')h_{2^{2n},b}(x')\mathrm{d}x'\mathrm{d}b \tag{16}$$

III. 2-D Fractional Wavelet Transform

A. 2-D FWT

The definition of 2-D FWT [21] is presented by synthesizing FWT [20] and 2-D WT, which is base on the WT and FRFT [22]. The 2-D FWT of the signal $f(x,y)$ can be defined as follows:

$$W\left(a_{mn},\bar{b}\right)=\iiiint B_{p1,p2}(x,y;x',y')f(x,y)\times h^{*}_{a_{mn}\bar{b}}(x',y')\mathrm{d}x\mathrm{d}y\mathrm{d}x'\mathrm{d}y' \tag{17}$$

In the fractional domains it can be written as:

$$W\left(a_{mn},\bar{b}\right)=\left(a_m a_n\right)^{1/2}\iint H^{*}\left(a_m u,a_n v\right)\times\exp\left(\mathrm{j}2\pi u b_{x'},\mathrm{j}2\pi v b_{y'}\right)\times F\left\{F^{\phi_1,\phi_2}\left[f(x,y)\right](x',y')\right\}(u,v)\mathrm{d}u\mathrm{d}v \tag{18}$$

where $h_{a_{mn}\bar{b}}(x',y')$ are the scaled and shifted wavelet functions of mother wavelet function, $a_{mn}=(a_m,a_n)$ is the discrete scaling vector, $\bar{b}=\left(b_{x'},b_{y'}\right)$ is the shift vector, $p=[p1,p2]$, $p1$ and $p2$ are the fractional orders.

While the back-reconstructing formula in the fractional domains is:

$$f(x,y)=\frac{1}{C}\iint F\{\sum\sum\iint\frac{1}{a_m a_n}W\left(a_{mn},\bar{b}\right)\times H\left(a_m u,a_n v\right)\exp\left(-\mathrm{j}2\pi u b_{x'},-\mathrm{j}2\pi v b_{y'}\right)\times\mathrm{d}b_{x'}\mathrm{d}b_{y'}\}\left(x',y'\right)B_{-p_1,-p_2}\left(x,y;x',y'\right)\mathrm{d}x'\mathrm{d}y' \tag{19}$$

B. 2-D FWT Calculation Steps

The calculation steps of 2-D FWT are shown as Fig. 2. As image decomposes, p order 2-D FRFT and the 2-D WT are used in sequence. As image reconstructs, the 2-D inverse wavelet transform (IWT) and $-p$ order 2-D FRFT are used in sequence.

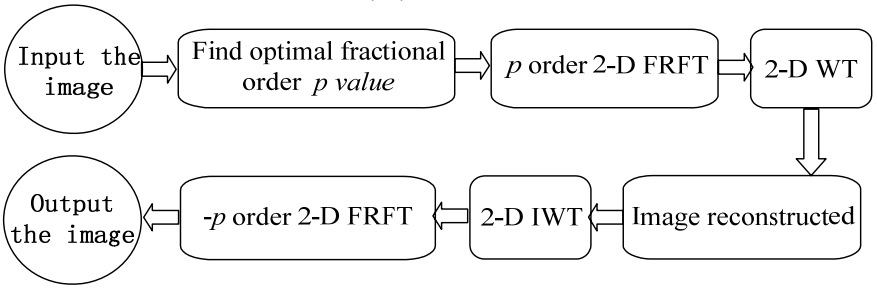

Figure 2. 2-D FWT calculation steps

The image with additive noise can be represented by:

$$\hat{X}(i,j)=X(i,j)+N(i,j) \tag{20}$$

where $X(i,j)$, $N(i,j)$ denote the image signal and noise signal respectively.

According to the superposition principle in linear transformation, the 2-D FWT of the signal with two additive and independent signals is equal to the sum of each 2-D FWT. Therefore, take the 2-D FWT of both sides in (20):

$$\hat{X}_p(u,v)=X_p(u,v)+N_p(u,v) \tag{21}$$

where $\hat{X}_p(u,v)$, $X_p(u,v)$ and $N_p(u,v)$ denote the 2-D FWT of $\hat{X}(i,j)$, $X(i,j)$ and $N(i,j)$ respectively.

The procedure of 2-D FWT-based image denoising method is given as follows.

- **Step1.** Giving the noise image $\hat{X}(i,j)$, and then find optimal fractional order p to reach the maximum Peak Signal to Noise Ratio (PSNR);
- **Step2.** Taking 2-D FWT of the noise image $\hat{X}(i,j)$, map into the optimal fractional wavelet domain, the image in fractional wavelet domain is obtained by (21).
- **Step3.** The image $\hat{X}_p(u,v)$ is denoised in the optimal fractional wavelet domain;
- **Step4.** Taking $-p$ order 2-D FRFT of the image, the denoised image can be obtained.

IV. Noise Estimation

A. Evaluation Indicators of Image Denoising

Evaluation standard of images quality is often described by the Peak Signal to Noise Ratio (PSNR) [23], and the PSNR is defined as:

$$PSNR=-10\lg\left(\frac{\sum_{i=1}^{m}\sum_{j=1}^{n}(X(i,j)-\hat{X}(i,j))^2}{m\times n\times 255^2}\right) \tag{22}$$

where $X(i,j)$ is the original image, $\hat{X}(i,j)$ is the estimate image after denoising, m and n are the row dimension and column dimension of the image respectively.

Higher *PSNR* means the denoised image is approximate to the original image, and the method has

better denoising effectiveness. In practice, a good denoising method can be found by visual effect and indicators of image denoising.

B. Noise Estimation

Images are often corrupted with noise, and the original image $X(i, j)$ is unknown in practice. Therefore, it is impossible to calculate the *PSNR* by (11), and then the optimal fractional order p can't be acquired without the optimal *PSNR*. To obtain the original image $X(i, j)$, the noise must be estimated firstly. In this paper, we mainly discuss the estimation of zero mean white Gaussian noise σ which has no relation with the images.

Research of noise estimation algorithms mainly focus on avoiding considering texture and edge information as noises. There are several traditional methods of noise estimation σ as bellows: One of the traditional methods is by subtracting the denoised image from the noising image. Usually, this method requires filters which can effectively remove the noise and preserve better edge details for the image. Another method is the noise image is taken apart into several pieces, and then separately estimates every part σ; take proper value as estimated value better. The third method is according to image statistical property to estimate image noise σ.

With the wide application of WT, the σ can be acquired by using the feature of image wavelet coefficients. The noise estimation method based on image wavelet coefficients is superior to the above. As the image is transformed into wavelet domain by WT, the large scale frequency coefficients have the main energy, and little energy exist in the high frequency with small amplitude. Thus, if the image has much noise, the coefficients of the highest frequency are considered as noises, and the σ can be estimated. Donoho et al. [24] have proved that noise variance is proportional to wavelet threshold, indicated that an accurate estimation of noise variance has an important influence on denoising effectiveness, and presented a noise estimation method by using the median amplitude of diagonal high-frequency wavelet coefficients, which is expressed as *MAD*. Then the noise variance can be calculated by (23).

$$\hat{\sigma} = MAD / 0.6745 \tag{23}$$

V. Optimal Fractional Order of 2-D FWT

The selection of the optimal fractional order p is a vital step in image denoising by 2-D FWT, and the select principle is to obtain the optimal *PSNR* after filter. However, the original image $X(i, j)$ is needed to calculate the objective evaluation standard *PSNR* by (22). As images are often corrupted with noise in acquisition and transmission process, and the noise is uncertain, the original image $X(i, j)$ can not be obtained.

To tackle the puzzle, a method of select the optimal fractional order p is presented in this paper, which is based on noise estimation. Mean Squared Error with Unknown Input Noise (*MSEUIN*) and Peak Signal to Noise Ratio with Unknown Input Noise (*PSNRUIN*) are proposed as the new evaluation standards of image denoising. The definitions of *MSEUIN* and *PSNRUIN* are given by (24) and (25) respectively.

$$MSEUIN = \frac{1}{m \times n} \sum_{i=1}^{m} \sum_{j=1}^{n} (Y(i, j) - \hat{N}(i, j) - \hat{X}(i, j))^2 \tag{24}$$

$$PSNRUIN = -10 \lg \left(\frac{\sum_{i=1}^{m} \sum_{j=1}^{n} (Y(i, j) - \hat{N}(i, j) - \hat{X}(i, j))^2}{m \times n \times 255^2} \right) = -10 \lg \frac{MSEUIN}{255^2} \tag{25}$$

where $Y(i, j)$ is input image with unknown noise, $\hat{X}(i, j)$ is the estimate image after denoising, and $\hat{N}(i, j)$ is estimation noise.

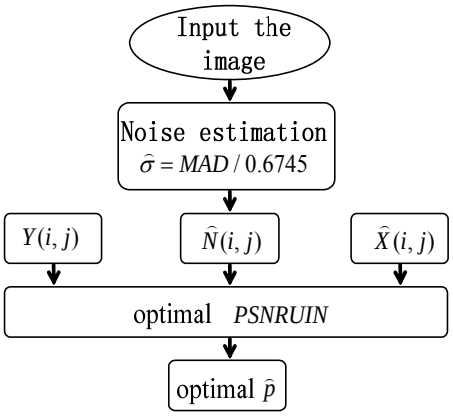

Figure 3. The selection process of the optimal fractional order $\hat{p}$ based on *PSNRUIN*

The closer $\hat{N}(i, j)$ matches actual noise $N(i, j)$, the closer $Y(i, j) - \hat{N}(i, j)$ matches the original image without noise $X(i, j)$. If $\hat{N}(i, j)$ equals $N(i, j)$, *PSNRUIN* equals *PSNR*. Likewise, the smaller the *MSEUIN*, the bigger the *PSNRUIN* and the closer estimate image $\hat{X}(i, j)$ match $X(i, j)$, the better effect of image denoising is achieved. Therefore, the fractional order p corresponding to the maximum *PSNRUIN* is represented as the estimate of optimal fractional order $\hat{p}$. The selection process of $\hat{p}$ based on the *PSNRUIN* is shown as Fig. 3.

VI. Experimental Results

A. Noise Estimation

Take lena image for example. The variance of the input white Gaussian noise σ is set as 10:10:90. The noise estimation method based on the median amplitude of diagonal high-frequency wavelet coefficients is adopted. The mother wavelet is sym4, the image is decomposed into two frequencies by 2-D FWT, and the front diagonal high-frequency wavelet coefficients is

picked up. The simulation results of noise estimation are listed in Table I.

TABLE I.
NOISE ESTIMATION OF LENA IMAGE.

σ	$\hat{\sigma}$	**error**
10	10.37	-3.7%
20	20.06	-0.3%
30	29.67	1.1%
40	38.68	3.3%
50	47.10	5.8%
60	55.35	7.8%
70	62.21	11.1%
80	69.20	13.5%
90	74.83	16.9%

Table I indicates the variance of image noise can be effectively estimated by using the proposed method. Especially, as the σ ranges from 10 to 40, the errors are within ± 5%. Therefore, the objective data obtained by the proposed method can be used to evaluate image quality accurately.

B. Selection of the Optimal Fractional Order

To demonstrate the validity of the proposed method of selecting the optimal fractional order $\hat{p}$ based on *PSNRUIN* empirically, we have conducted simulations on lena image with white Gaussian noise. The variance of the input white Gaussian noise σ is set as 10:10:90. The simulation results are given in Table II. As σ equals 40, denoising effectiveness of p acquired by *PSNR* and $\hat{p}$ acquired by *PSNRUIN* is shown in Fig. 4.

In the simulations, the noised image is decomposed with wavelet firstly. From (23), the estimate for noise variance $\hat{\sigma}$ can be calculated by the median amplitude of diagonal high-frequency wavelet coefficients (*MAD*) and zero mean white Gaussian noise $\hat{N}(i,j)$ is achieved. Then, $\hat{X}(i,j)$ denoised by $\hat{p}$ order FWT, the estimate of white Gaussian noise $\hat{N}(i,j)$ and noised image $Y(i,j)$ are used to calculate *PSNRUIN* . The order value corresponding to the maximum *PSNRUIN* as it ranges from 0 to 1 is the optimal fractional order $\hat{p}$. Here, the soft-threshold function is adopted in 2-D FWT analysis. By using different wavelet basis function db3, db4, db5, db6, db7,db8 and the image decomposed into 2, 3, and 4 frequency bands respectively, thus there have been different *PSNR* corresponding to each case and the maximal *PSNR* is determined.

In Table II, wname and level represent the wavelet basis function and the number of decomposed bands corresponding to the maximum *PSNR* respectively. The *PSNR* is calculated by using the optimal fractional order with known noise, and *PSNRP* is the *PSNR* corresponding to the optimal fractional order $\hat{p}$. The error between *PSNRP* corresponding to $\hat{p}$ and *PSNR* corresponding to p is given as (26).

$$error = \frac{PSNR - PSNRP}{PSNR} \tag{26}$$

TABLE II.
THE SELECTION OF THE OPTIMAL FRACTIONAL ORDER $\hat{p}$ BASED ON 2-D FWT DENOISING OF LENA IMAGE

σ	**wname**	**level**	p **×100**	**PSNR**
10	db8	2	[0,0]	30.28
20	db8	2	[4,4]	28.64
30	db8	2	[5,5]	27.51
40	db8	2	[5,6]	26.36
50	db8	3	[2,1]	24.94
60	db8	3	[2,2]	24.53
70	db8	3	[2,2]	24.01
80	db8	3	[2,2]	23.42
90	db7	3	[2,2]	22.89

TABLE II. （CONTINUED）

σ	$\hat{\sigma}$	$\hat{p}$ **×100**	**PSNRUIN**	**PSNRP**	**error**
10	10.44	[0,0]	21.29	30.28	0
20	20.06	[4,4]	19.12	28.64	0
30	29.85	[5,5]	17.06	27.51	0
40	38.83	[6,6]	15.30	26.36	0
50	47.54	[2,1]	13.51	24.94	0
60	55.39	[2,2]	12.36	24.53	0
70	62.34	[2,2]	11.43	24.01	0
80	69.20	[2,3]	10.64	23.39	0.13%
90	74.51	[3,3]	10.01	22.82	0.31%

(a) Orginal lena image with no noise

(b) Lena image with white Gaussian noise

(c)Denoising result base on 2-D FWT as p = [5,6]

(d) Denoising result base on 2-D FWT as $\hat{p}$ = [6,6]

Figure 4. Denoising of the lena image

In Table II, the p and $\hat{p}$ are approximately equal. The difference between p and $\hat{p}$ exists when $\sigma \geq 80$ and the error between *PSNR* and *PSNRP* is within 0.5%. As Fig. 4 suggests, there is a negligible difference in denoising effectiveness between p and $\hat{p}$. According these comparative experiments, the proposed method used to select the optimal fractional order p of image with unknown noise is accurate and effective.

Besides, to confirm whether the proposed method of the optimal fractional order $\hat{p}$ based on the *PSNRUIN* can also apply to 2-D FRFT denoising, simulated results of the lena image with white Gaussian noise by using 2-D FRFT are shown in Table III.

TABLE III

THE SELECTION OF THE OPTIMAL FRACTIONAL ORDER $\hat{p}$ BASED ON 2-D FRFT DENOISING OF LENA IMAGE

σ	p ×100	PSNR	$\hat{p}$ ×100	PSNRUIN	PSNRP	error
10	[97,100]	32.25	[93,92]	26.33	31.46	2.45%
20	[95,97]	29.89	[91,91]	21.14	28.52	4.58%
30	[95,95]	27.66	[90,89]	17.86	25.46	7.95%
40	[94,94]	25.79	[89,88]	15.58	23.33	9.54%
50	[94,94]	24.32	[88,88]	13.90	21.92	9.87%
60	[94,93]	22.96	[87,87]	12.61	20.18	12.11%
70	[94,93]	21.92	[87,86]	11.59	19.14	12.68%
80	[93,93]	20.94	[86,86]	10.81	18.23	12.94%
90	[94,92]	20.24	[86,85]	10.12	17.40	14.03%

As shown in Table III, there are different values between p and $\hat{p}$, which indicates the estimator $\hat{p}$ for p is inaccurate by using the proposed method based on *PSNRUIN*. With the increase of noise σ, the error between *PSNR* and *PSNRP* increases, and the error is within 10% when σ <50. Therefore, the method of the optimal fractional order $\hat{p}$ based on *PSNRUIN* used to estimate the optimal fractional order p for image denoising with unknown noise by 2-D FRFT is unfavourable.

VII. CONCLUSIONS

With the development of time-frequency image processing, FWT theory and its application in image processing increasingly draw experts and scholar's attention. Aiming to the image with unknown noise in practice, Peak Signal to Noise Ratio with Unknown Input Noise (*PSNRUIN*) is considered as the evaluation standards of image denoising, and the optimal fractional order can be calculated according to the *PSNRUIN* .

ACKNOWLEDGMENT

The authors wish to thank Youren Wang, Hui Luo. This work is supported by the National Natural Science Foundation of China (No. 60871009), Aviation Science Foundation of China (No. 2011ZD52050), Fundamental Research Funds for the Central Universities (No. CXLX11_0183), Natural Science Foundation of Anhui

education department (No. KJ2012B062). The authors are grateful for editors and anonymous reviewers who made constructive comments.

REFERENCES

[1] J. Tian, L. Chen and L. Ma, "A wavelet-domain non-parametric statistical approach for image denoising," *IEICE Electronics Express*, vol.7, no.18, pp.1409-1415, 2010.

[2] A. Buades, B. Coll and J.-M. Morel, "A non-local algorithm for image denoising," *IEEE Computer Society Conference on Computer Vision and Pattern Recognition*, vol.2, pp. 60-65, June 2005.

[3] T. Brox , O. Kleinschmidt and D. Cremers, "Efficient nonlocal means for denoising of textural patterns," *IEEE Trans. Image Process*, vol. 17, no. 7, pp. 1083-1092, 2008.

[4] L. Rudin, S. Osher and E. Fatemi, "Nonlinear total variation based noise removal algorithms," *Phys. D*, vol. 60, no. 1–4, pp. 259-268, 1992.

[5] A. Chambolle, "An algorithm for total variation minimization and applications," *Journal of Mathematical imaging and vision*, vol. 20, no. 1/2, pp. 89-97, 2004.

[6] P. Liu , D. Liu and Z. Liu, "Total variation restoration of the defocus image based on spectral priors," *Proc. SPIE*, vol. 7830,, October 2010.

[7] F. Abramovitch, T. Sapatinas and B. W. Silverman, "Wavelet thresholding via a Bayesian approach," *Journal of the Royal Statistical Society: Series B (Statistical Methodology)*, vol. 60, no. 4, pp. 725-749, 1998.

[8] L. Sendur and I. W. Selesnick, "Bivariate shrinkage functions for wavelet-based denoising exploiting interscale dependency," *IEEE Trans. Signal Process*, vol. 50, no. 11, pp. 2744-2756, 2002.

[9] J. Portilla, V. Strela, M. J. Wainwright and E. P. Simoncelli, "Image denoising using scale mixtures of gaussians in the wavelet domain," *IEEE Trans. Image Process*, vol. 12, no. 11, pp. 1338-1351, 2003.

[10] F. Luisier and T. Blu, "SURE-LET multichannel image denoising: Interscale orthonormal wavelet thresholding," *IEEE Trans. Image Process*, vol. 17, no. 4, pp. 482-492, 2008.

[11] P. Scheunders and S. De Backer, "Wavelet denoising of multicomponent images using gaussian scale mixture models and a noise-free image as priors, image processing," *IEEE Trans. Image Process*, vol. 16, no. 7, pp. 1865-1872, 2007.

[12] P. Liu, F. Huang, G. Li and Z. Liu, "Remote-Sensing Image Denoising Using Partial Differential Equations and Auxiliary Images as Priors," *IEEE Geoscience and Remote Sensing Letters*, vol. 9, no.3, pp.358-362, 2012.

[13] M. R. Portnoff, "Time-frequency representation of digital signals and systems based on short-time Fourier analysis," *IEEE Trans. Acoust., Speech, Signal Process*, vol. ASSP-28, no. 1, pp. 55-69, Feb. 1980.

[14] S.G. Mallat, "A theory for multiresolution signal decomposition: The wavelet representation," *IEEE Trans. Pattern Anal. Mach. Intell.*, vol. 11, no. 7, pp.674-693, 1989.

[15] G. Bhatnagar, Q. M. J. Wu and B. Raman, "A New Fractional Random Wavelet Transform for Fingerprint Security," *IEEE Transactions on Systems, Man and Cybernetics, Part A: Systems and Humans*, vol. 42, no. 1, pp. 262-275, 2012.

[16] B. Pesquet-Popescu and A.Kaup, "Methods and tools for wavelet-based scalable multiview video coding," *IEEE Transactions on Circuits and Systems for Video Technology*, vol.21, no.2, pp.113-126, 2011.

[17] N. Terzija and H. Mccann, "Wavelet-based image reconstruction for hard-field tomography with severely limited data," *IEEE Sensors Journal*, vol. 11, no. 9, pp.1885-1893, 2011.

[18] Hui Luo, Y. Wang, Jiang Cui., "A SVDD approach of fuzzy classification for analog circuit fault diagnosis with FWT as pre-processor," *Expert Systems with Applications*, vol. 38, no. 8, pp.10554-10561, 2011.

[19] G. Bhatnagar, Q.M. Jonathan Wu and B. Raman, "Discrete fractional wavelet transform and its application to multiple encryption," *Information Sciences*, vol. 223, pp.297-316, February 2013.

[20] D. Mendlovic, Z. Zalevsky, D. Mas, J. García and C. Ferreira, "Fractional wavelet transform," *Applied Optics*, vol. 36, no.20, pp.4801-4806, 1997.

[21] Lin-fei Chen and Dao-mu Zhao, "Optical image encryption based on fractional wavelet transform," *Optics Communications*, vol. 254, no. 4-6, pp.361-367, 2005.

[22] Ran Tao, Bing Deng and Yue Wang, "Research progress of fractional Fourier transform in signal processing," *Science in China Ser. E Information Sciences*, vol. 36, no. 2, pp.113-136, 2006.

[23] S.D. Backer, A. Pižurica, B. Huysmans, W. Philips and P. Scheunders, "Denoising of multicomponent images using wavelet least-squares estimators," *Image and Vision Computing*, vol. 26, no. 7, pp.1038-1051, 2008.

[24] D.L. Donoho, I. Johnstone, G. Kergyacharian and D. Picard, "Density estimation by wavelet thresholding," *Annals of Statistics*, vol. 24, no. 2, pp.508-538, 1996.

Yuanyuan Jiang was born in 1982. She received the B.S. degree in automation and M.S. degree in Power electronics and power transmission from Anhui University of Science and Technology, Huainan, China, in 2003 and 2006. She is currently working toward the Ph.D degree from Nanjing University of Aeronautics and Astronautics (NUAA), Nanjing, China. Her research interests are signal processing and electronic system prognostic.

Youren Wang was born in 1963. He received the B.S. degree in wireless engineering and M.S. degree in Circuits and Systems from Southeast University, Nanjing, China, in 1984 and 1987. He received the Ph.D degree in Power electronics technology from Nanjing University of Aeronautics and Astronautics (NUAA), Nanjing, China, in 1996. He is currently a professor and Ph.D. supervisor in College of Automation Engineering, NUAA, China. His teaching and researching interests include analog and digital circuits design, test, fault tolerant and prognostics, intelligent information on process, and evolvable hardware design.

Hui Luo was Born in 1982. She received the B.S. and M.S. degree in computer application technology from Anhui Industrial university, Maanshan, China, in 2004 and 2008. She received the Ph.D degree in Measurement & Test Techniques and Instrument from Nanjing University of Aeronautics and Astronautics, Nanjing, China, in 2012. Currently, she is working at Nanjing Agriculture University in China. Her main research interests include analog circuit test and measurement, and pattern recognition.